SCIENTIFIC REPORTS
natureresearch

OPEN

Highly *c*-axis orientated superconducting core and large critical current density in Ba$_{0.6}$Na$_{0.4}$Fe$_2$As$_2$ powder-in-tube tape

S. Imai[1,2], S. Itou[1,2], S. Ishida [2], Y. Tsuchiya[2], A. Iyo[2], H. Eisaki[2], K. Matsuzaki[2], T. Nishio[1] & Y. Yoshida[2]

Improvement of the critical current density (J_c) of superconducting wires/tapes is one of the key issues in the field of superconductivity applications. Here we report the fabrication of a silver-sheathed Ba$_{1-x}$Na$_x$Fe$_2$As$_2$ (BaNa-122) superconducting tape by using a powder-in-tube technique and its superconducting properties, in particular transport J_c, as well as the tape-core texture. The optimally-doped BaNa-122 tape with Na concentration $x = 0.4$ exhibits the superconducting critical temperature (T_c) of 33.7 K and high transport J_c of 4×10^4 A/cm^2 at 4.2 K in a magnetic field of 4 T. Patterns of x-ray diffraction for the superconducting core show that the degree of *c*-axis orientation is significantly enhanced through the tape fabrication process. The tendency of *c*-axis orientation is advantageous for achieving higher J_c, suggesting the high potential of BaNa-122 for superconducting wire/tape applications.

Since the discovery of the high-transition-temperature (high-T_c) superconductivity in iron-based superconductors (IBSs)[1], they have attracted much attention from the viewpoint of basic research as well as applications[2-5]. Among various types of IBSs, so-called 122-type materials represented as $AE_{1-x}A_x$Fe$_2$As$_2$ (AE: alkaline earth metal, A: alkali metal) have several characteristics suitable for applications[6-8]: the maximum T_c of 38 K, large upper critical fields (H_{c2}) exceeding 100 T, and small anisotropy ($\gamma = H_{c2}{}^{ab}/H_{c2}{}^{c} \sim 1$–2)[9,10]. In particular, K-doped ($A = K$) materials, i.e. Ba$_{1-x}$K$_x$Fe$_2$As$_2$ (BaK-122) and Sr$_{1-x}$K$_x$Fe$_2$As$_2$ (SrK-122), have been generally used for the fabrication of powder-in-tube (PIT) wires/tapes. The latest BaK-122 tapes possess the transport critical current density (transport J_c) of 1.5×10^5 A/cm^2 at 4.2 K and 10 T[11], which is over a level in practical use under this condition, while further improvement of J_c is required.

To date, massive efforts have been devoted to improve the fabrication process of wires/tapes toward higher J_c. It has been established that J_c values can be significantly increased when a uniaxial pressing is applied to tapes after the flat-rolling process. The application of uniaxial pressure is found to enhance the superconducting-core density as well as the *c*-axis alignment of the grains, which are considered to be correlated with J_c[11-17]. Accordingly, the enhancement of two factors, namely, the core density and the grain alignment, has been mainly focused to achieve higher J_c. Currently, the highest J_c was achieved for BaK-122 tapes fabricated by a hot-press technique[11]. Here, Huang *et al.*[11] argued that BaK-122 is more suitable for the PIT tapes compared with SrK-122 because a higher degree of *c*-axis orientation in the core, which was associated with the high J_c, was obtained through the same fabrication process. In addition, the Vickers hardness of the tape core, which is a measure of the core density, was smaller than that of 122 wires (no *c*-axis orientation)[18]. This suggests that the *c*-axis orientation becomes more important to achieve a practical-level J_c after obtaining a sufficiently high core density.

[1]Department of Physics, Tokyo University of Science, 1-3 Kagurazaka, Shinjuku, Tokyo, 162-8601, Japan. [2]National Institute of Advanced Industrial Science and Technology (AIST), 1-1-1 Umezono, Tsukuba, Ibaraki, 305-8568, Japan. Correspondence and requests for materials should be addressed to S.Imai (email: s.imai@aist.go.jp) or S.Ishida (email: s.ishida@aist.go.jp) or T.N. (email: nishio@rs.kagu.tus.ac.jp)
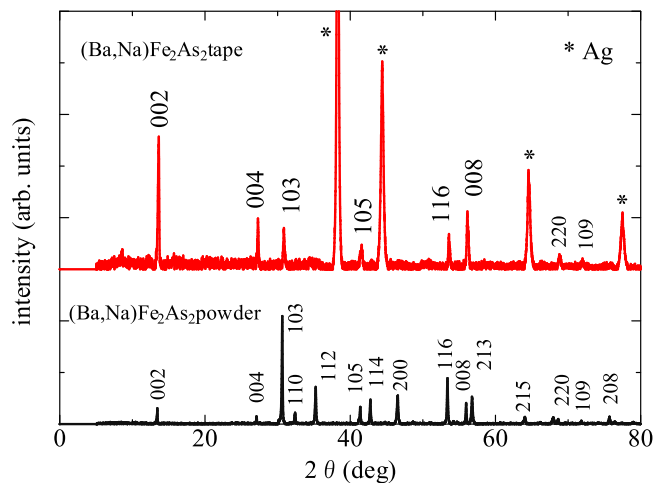
Figure 1. XRD patterns of randomly oriented BaNa-122 polycrystalline powder (black line) and the tape surface (red line). Asterisks indicate diffraction peaks from Ag sheath material.

Meanwhile, we fabricated PIT tapes using $Sr_{1−x}Na_xFe_2As_2$ (AE = Sr and A = Na; SrNa-122) and achieved a high transport J_c exceeding 1×10^4 A/cm² at 20 K under magnetic fields up to 2.5 T[19]. Interestingly, we found the precipitation of Ag-As alloys in the superconducting core of SrNa-122 tape after the heat treatment process, although Ag was not added to the starting powders. The precipitation of Ag-As alloys has not been reported for any other AEK-122 wires/tapes. The Ag-As alloys are likely conductive, hence they possibly improve the grain connectivity and thus contribute to the enhancement of J_c as discussed in previous studies where extra metals such as Sn, Pb, and Ag were added to the core[17,20].

These results in previous studies indicate that the choice of AE and A enhances/suppresses the c-axis alignment of the core and/or promotes the chemical reaction with sheath materials (Ag in the present case), and thus affects J_c of 122-based PIT wires/tapes. In this study, we focus on the combination of AE = Ba and A = Na, namely, $Ba_{1−x}Na_xFe_2As_2$ (BaNa-122)[21], which is recently used for the PIT wire fabrication[22], while its potential for the PIT tape fabrication is unexplored. We obtained high J_c exceeding 4×10^4 A/cm² at 4.2 K under a magnetic field of 4 T. We found that the BaNa-122 tape core has a remarkably high degree of c-axis orientation by comparing the orientation factor with various BaK-122 and SrNa-122 tapes. We also found the precipitation of Ag-As alloys in the BaNa-122 tape core similarly to the case of SrNa-122 tape, while the amount of Ag-As precipitation is much smaller compared with SrNa-122. The Vickers hardness of the BaNa-122 tape core ($H_v \sim 90$) is relatively small, indicating that the low core density is the main limiting factor of J_c of the present BaNa-122 tape.

Results

X-ray diffraction analysis.
Figure 1 shows XRD patterns of the BaNa-122 polycrystalline powder (black) and tape (red) samples. All the visible peaks can be indexed based on the 122 structure (ThCr₂Si₂ type, I4/mmm). No impurity peaks were observed in the range of resolution. The lattice constants of the powder sample estimated from the d values of peaks are $a = 3.902$ Å and $c = 13.13$ Å. These values correspond to $x = 0.4$[21], indicating that the Na composition of the present powder was successfully controlled. The peak positions of XRD patterns of the superconducting core surface are almost identical to those for polycrystalline powders within the experimental certainty, indicating that the Na concentration was not significantly changed through the tape fabrication process. On the other hand, the intensities of the 00l peaks of tape core are largely enhanced in comparison with the polycrystalline powder. This indicates that the c-axis of BaNa-122 grains is well-oriented perpendicularly to the tape surface, that is, along the direction of the uniaxial pressure.

Magnetic susceptibility.
Figure 2 shows the temperature (T) dependence of magnetic susceptibility for polycrystalline powders (black) and a 3 mm-long tape (red) measured under the field of 10 Oe. The filled and open symbols indicate the data taken by the zero-field-cool and field-cool processes, respectively. The T_c values were determined as a temperature where the susceptibility dropped by 10% of the superconducting transition in the zero-field-cool branch. The determined T_c of the polycrystalline powder is 34.2 K, which is in good agreement with the reported T_c of BaNa-122 with $x = 0.4$[21], supporting that the Na concentration was successfully controlled. After the fabrication process, T_c (= 33.7 K) of the tape is found to decrease by 0.5 K from that of powder, while the width of superconducting transition is preserved.

The degradation in T_c after wire/tape fabrication process has been also reported in previous works[23]. An explanation for the reduction in T_c is the loss of Na during the fabrication process, although the Na concentration is seemingly unchanged within the resolution of the XRD and the EDX measurements. On the other hand, the reduction in T_c is possibly caused by the mechanical stress during the wire/tape fabrication process. It was pointed that T_c possibly decreases if the local structures such as pnictogen height and As-Fe-As bond angle are changed by the mechanical stress because T_c of IBSs is sensitive to these local structures.
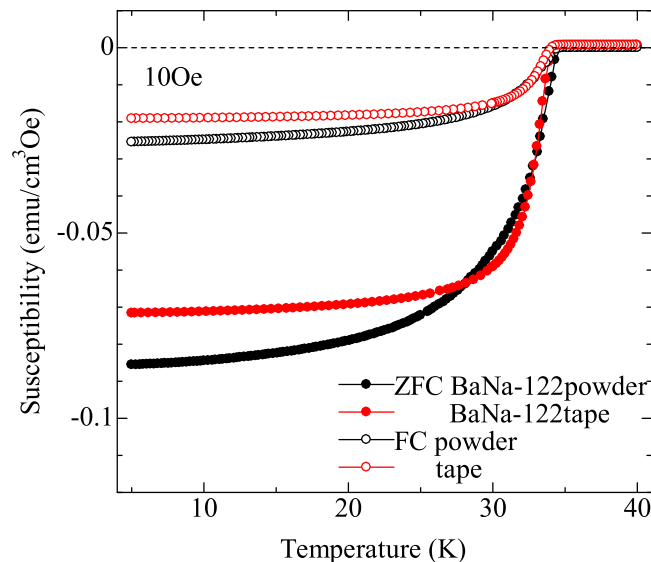
Figure 2. Temperature dependence of magnetic susceptibility of BaNa-122 powder (black) and tape (red) measured under the field of 10 Oe. The filled and open symbols indicate the data taken by the zero-field-cool and field-cool processes, respectively.
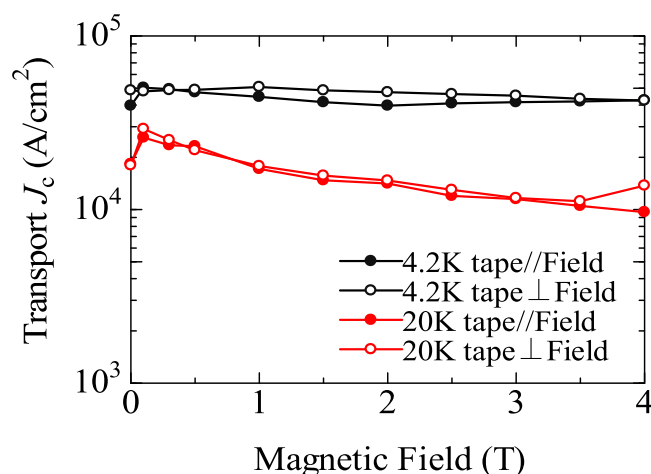

Figure 3. Magnetic field dependence of transport J_c of a (Ba, Na)Fe$_2$As$_2$ tape at 4.2 K (black) and 20 K (red) under magnetic fields up to 4 T applied parallel (closed circles) and perpendicular (open circles) to the tape surface.

Transport J_c. Figure 3 shows the magnetic field (H) dependence of transport J_c. The measurements were performed at 4.2 K (black) and 20 K (red) under magnetic fields up to 4 T applied parallel (filled circles) and perpendicular (open circles) to the tape surface. At $T = 4.2$ K and H // tape surface, the BaNa-122 tape shows a large transport J_c values of 5.0×10^4 A/cm^2 and 4.3×10^4 A/cm^2 under self-field and 4 T, respectively. The high J_c is maintained even at 20 K; J_c values are 1.5×10^4 A/cm^2 under a self-field and 1.0×10^4 A/cm^2 under 4 T. Moreover, J_c curves exhibit weak H dependence with a ratio $J_c(0\,\text{T})/J_c(4\,\text{T}) \sim 1.4–1.5$. Furthermore, J_c values under the magnetic fields parallel and perpendicular to the tape surface are almost identical to each other, or J_c is even slightly higher for H perpendicular to the tape surface.

SEM-EDX analysis. Figure 4(a,b) show SEM images of the cross section of the BaNa-122 tape core obtained at different magnifications. EDX analyses show that the average atomic composition in the core, Ba: Na: Fe: As, is approximately 12: 8.8: 37: 40. This atomic ratio corresponds to (Ba$_{0.62}$Na$_{0.43}$)Fe$_{1.8}$As$_{2.0}$, indicating that the Na concentration is ~0.4, which is close to the nominal composition of the starting powder. The SEM images show the presence of Fe$_2$As impurities (dark gray spots), which are not detected by the XRD measurements. The amount of Fe$_2$As was estimated to be ~3.7% from the cross-section area of the SEM images. The black regions correspond to voids or cracks with the sizes of a few micrometers. Such voids/cracks have been considered as one of the main
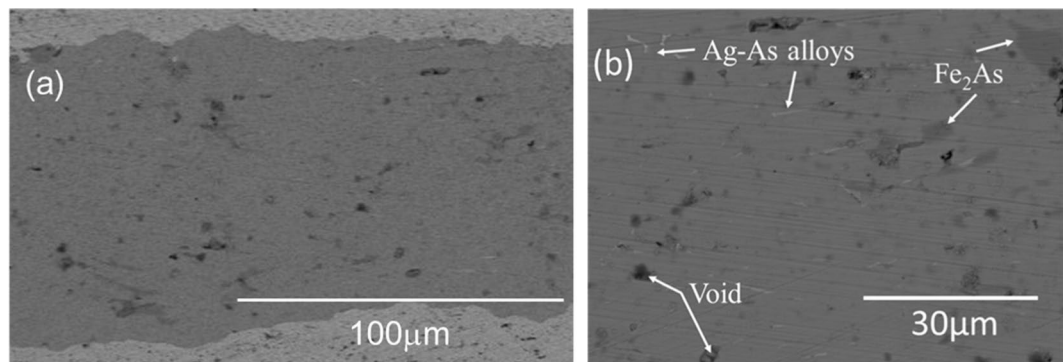
Figure 4. (**a,b**) SEM images of the cross section of a BaNa-122 tape taken at different magnifications.
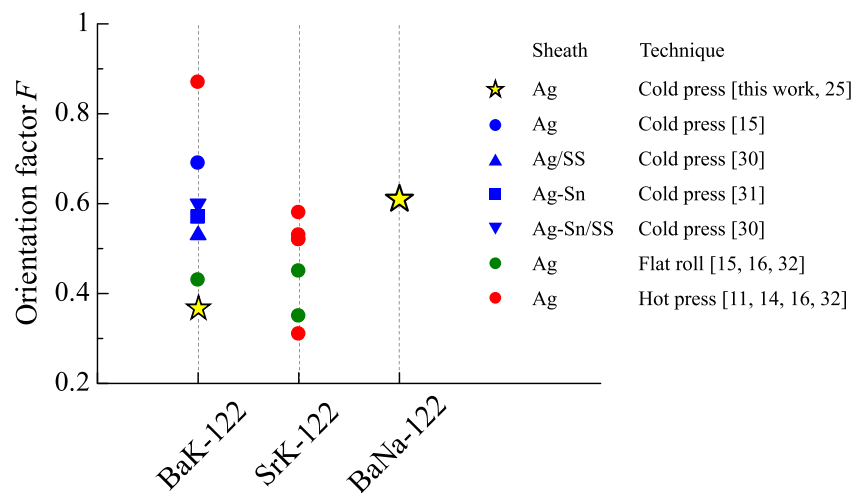
Figure 5. Orientation factor F of BaK-122[11,15,25,30,31], SrK-122[14,16,32], and BaNa-122. Several F values were calculated using the XRD patterns given in the references. The symbols indicate the sheath materials and techniques used for the tape fabrication process.

limiting factors of J_c. The blight rod-like spots are found to be Ag-As alloys. Note that Ag was not added to the starting powders and a similar phenomenon was reported for the SrNa-122 tape[19].

Discussion

A high-performance IBS tape was successfully fabricated by using BaNa-122, demonstrating that BaNa-122 is also a good candidate material for superconducting wire/tape applications. In particular, an advantageous characteristic is found, i.e. the superconducting core of the BaNa-122 tape is strongly c-axis oriented perpendicularly to the tape surface. Note that the high c-axis orientation has been considered as an important factor for improving J_c[14,15]. To quantify the degree of c-axis orientation, the orientation factor (F) was estimated based on the XRD patterns by using the Lotgering method[24], i.e. $F = (\rho - \rho_0)/(1 - \rho_0)$ with $\rho = \Sigma I(00\,l)/\Sigma I(hkl)$ and $\rho_0 = \Sigma I_0(00l)/\Sigma I_0(hkl)$, where $I(hkl)$ ($I_0(hkl)$) is the intensity of the hkl peak for tapes (polycrystalline powders). The estimated F of the present BaNa-122 tape is 0.61. This value is larger than that of our BaK-122 tape ($F = 0.37$)[25], suggestive of a better c-axis orientation of the BaNa-122 core. For further comparison, in Fig. 5, we plotted the F values of various BaK-122 and SrK-122 tapes taken from references. The F value of the BaNa-122 tape is found to be considerably high among those of 122 tapes. It should be noted that the high F values (>0.5) of previous BaK-122 and SrK-122 tapes were achieved using advanced techniques efficient for obtaining the c-axis orientation; (i) application of large uniaxial pressure (~4 GPa, which is 4 times larger than that in this work), (ii) application of hot-press technique, or (iii) use of Ag-Sn alloy sheath or Ag/stainless steel (SS) double sheath (which are harder than the pure Ag sheath used in this work). Thus, the comparison of F values between the BaNa-122 tape and various BaK-/SrK-122 tapes demonstrates that the use of BaNa-122 material is promising for obtaining a better c-axis orientation of the tape core.

The high c-axis orientation found for the BaNa-122 core is possibly associated with the strain in the crystal structure. It is reported that the c axis of BaNa-122 shows a non-monotonic x dependence violating the Vegard's law (the c-axis parameter increases up to $x \sim 0.4$ while decreases at higher x) owing to the large mismatch of ionic radii between Ba^{2+} and Na^{+}[26]. This suggests that BaNa-122 has a significant strain in the crystal structure compared with other 122 materials, which possibly causes an easy cleavage of the grains during the flat-rolling and

uniaxial-pressing processes. Such cleaved grains likely align easily and thus result in the high c-axis orientation of the tape core.

In addition, the precipitation of Ag-As alloys was observed in the BaNa-122 tape core similarly to the case of SrNa-122 tape[19], which has not been reported for K-doped 122 tapes. The Ag-As alloys occupy about 0.6% of the cross-section area for the present BaNa-122 tape, which is smaller than that estimated for the previous SrNa-122 tape (~3%). Meanwhile, the amount of Fe_2As impurities is also smaller for BaNa-122 (~3.7%) than that for SrNa-122 tape (~10%). For BaK-122 and SrK-122, the Ag-As alloys have not been observed and the amount of Fe_2As impurities is much smaller. There seems a correlation between the amounts of Ag-As alloys and Fe_2As impurities, suggesting that the precipitation of Ag-As alloys is the resultant of the chemical reaction between 122 phase and the Ag sheath. The degree of chemical reaction between 122 and Ag sheath is possibly associated with the chemical stability of 122 phase. Note that AENa-122 phase has a solubility limit at some Na concentration because Na-122 ($x = 1$) is a metastable phase[21,27,28], while AEK-122 phase can be obtained for any K concentration. Therefore, AENa-122 is likely more unstable and hence reactive compared with AEK-122. In addition, SrNa-122 used for the tape contains a higher Na concentration than that of BaNa-122 because T_c is optimized at $x = 0.55$ and 0.4 for SrNa-122 and BaNa-122, respectively. Then, SrNa-122 is closer to the solubility limit hence more unstable compared with BaNa-122. Thus, the precipitation of Ag-As alloys is most prominent for the most unstable SrNa-122 core.

Regarding the Ag-As precipitation, two opposing effects on the grain connectivity, which is one of the key factors determining J_c, are considered; (i) the Ag-As alloys fill voids and cracks in the core and thus improve the grain connectivity, and (ii) the accompanying Fe_2As impurities disturb the grain connectivity. Then, J_c is possibly increased by balancing the positive and negative effects. For the optimization of the precipitation of Ag-As alloys and Fe_2As impurities, the fine adjustments of the heat-treatment temperature and time as well as the chemical composition of the BaNa-122 powder should be considered.

Meanwhile, the transport J_c of the present BaNa-122 tape does not reach the practical-level J_c ($= 10^5\,A/cm^2$) in spite of the considerably high F value. To understand the limiting factor of J_c, we checked the Vickers hardness (H_V) of the BaNa-122 core, which is often used as a measure of the core density. The obtained $H_V \sim 90$ is relatively small compared with the other 122 tapes with higher J_c. Therefore, we concluded that the low core density owing to the presence of crack and voids mainly limits J_c of the present BaNa-122 tape. Such cracks and voids are expected to be reduced by using the techniques mentioned above, i.e. application of a large uniaxial pressure, hot press, and hard sheath materials. Note that these techniques are also efficient for the enhancement of c-axis orientation. Thus, the use of BaNa-122, which provides a better c-axis orientation, possibly leads to the further enhancement of J_c of 122-based PIT tapes. On the other hand, it should be also noted that the cold- and hot-press techniques limit the length of the tape hence they are not suitable for the mass production (in the present study, the length of the tape (~50 mm) is limited by the uniaxial-press process). Then, the application of hot rolling and over-pressure sintering, which have been used for the production of high-T_c BSCCO tapes, should be interesting in terms of the scale up of the tape length.

Finally, regarding the H dependence of transport J_c of the present BaNa-122 tape, a weak H dependence and a small anisotropy against the H orientation were observed similarly to BaK-122 and SrK-122 tapes, which are important properties from the application viewpoint. Note that the J_c anisotropy is smaller than (or inversed from) that expected from the anisotropy of H_{c2}, namely, the effective mass model. The inverse anisotropy has been also reported for BaK-122[11] and SrK-122 tapes[29]. To account for this behavior, two scenarios have been proposed; (i) correlated pinning centers, i.e. elongated perpendicular to the tape surface, or (ii) pinning centers larger than the coherence length dominate the pinning properties. To elucidate the origin of the inverse anisotropy of J_c, it is desired to perform the transmission-electron-microscopy measurement, which is a powerful tool to investigate the defect structures determining vortex pinning properties.

Summary

An iron-based superconducting PIT tape was fabricated using BaNa-122. High J_c values of $5.0 \times 10^4\,A/cm^2$ at 4.2 K under a self- field and $1.0 \times 10^4\,A/cm^2$ at 20 K under a magnetic field of 4 T were achieved, which are comparable to those in BaK-122 and SrK-122 tapes. Also, a weak H dependence of J_c and a small anisotropy of J_c against the H orientation were observed similarly to the cases of BaK-122 and SrK-122 tapes, which are important properties for high-field applications. Moreover, we found an advantageous characteristic of BaNa-122 tape; the superconducting core tends to show a high c-axis orientation. Meanwhile, a substantial amount of voids and cracks are observed in the core, which are likely to be the main limiting factor of the transport J_c of present BaNa-122 tape. Then, there still remains room for the further enhancement of J_c in BaNa-122 tapes by taking advantage of the better c-axis orientation.

Methods

Polycrystalline powders of BaNa-122 were synthesized by a solid-state reaction. Prior to the synthesis, BaAs, NaAs, and Fe_2As powders were prepared as precursors by mixing elemental Ba, Na, Fe, and As chunks at stoichiometric molar ratio, sealing them into quartz tubes (BaAs and Fe_2As) or stainless-steel container (NaAs), and heating at 650 °C (BaAs and NaAs) and 750 °C (Fe_2As). The precursors were mixed in the ratio of BaAs: NaAs: $Fe_2As = 0.6$: 0.45: 1. Here, the target Na concentration was $x = 0.4$ so as to yield highest T_c of 34.2 K. Extra NaAs was added considering the possible loss of Na and As during the synthesis process. The mixed powders were put in an alumina crucible and then sealed in a stainless-steel container, then sintered at 770 °C for 15 hours. The polycrystalline powders were pressed into a pellet by applying a pressure of about 100 MPa. The pellet was packed into a silver tube having an outer diameter of 10 mm and an inner diameter of 4.3 mm. The silver tube was groove-rolled into a square wire with the $1.2 \times 1.2\,mm^2$ cross-sectional and subsequently flat-rolled into a tape with a thickness of 0.48 mm. The flat rolled tape was uniaxial cold-pressed between stainless steel disks under a

pressure of approximately 1.0 GPa. After this press process the thickness of tape was reduced to 0.20 mm. The thin tape was cut into 50 mm long pieces, sealed into a stainless-steel container in a N_2-filled glove box, and sintered at 875 °C for 3 h.

Measurements of x-ray diffraction (XRD) for polycrystalline powders and superconducting tape cores were performed at room temperature using Cu K_α radiation (the peaks from Cu $K_{\alpha 2}$ were removed using Peak search, Rigaku Corporation). Magnetic susceptibility was measured by using a SQUID magnetometer (Quantum design, MPMS). The cross section of the superconducting core was examined with a scanning electron microscope SEM (Hitachi High-Technologies TM3000) and the composition analysis was carried out by an energy dispersive x-ray EDX spectrometer (Oxford Instruments SwiftED 3000). Vickers hardness (H_V) was measured on the polished surface of the tape core using a Micro Vickers hardness testing machine (Matsuzawa MMT-X3). Five different positions were measured with a 25 g load and 10 s duration, and an average value was calculated. Transport critical current (I_c) measurements were performed by using a four-terminal method at 4.2 K and 20 K under magnetic fields up to 4 T.

References

1. Kamihara, Y. *et al.* Iron-based layered superconductor La[O$_{1-x}$F$_x$]FeAs (x = 0.05–0.12) with T_c = 26 K. *J. Am. Chem. Soc.* **130**, 3296–3297 (2008).
2. Hosono, H. & Kuroki, K. Iron-based superconductors: Current status of materials and pairing mechanism. *Phys. C Supercond. its Appl.* **514**, 399–422 (2015).
3. Hosono, H., Yamamoto, A., Hiramatsu, H. & Ma, Y. Recent advances in iron-based superconductors toward applications. *Mater. Today* **21**, 278–302 (2018).
4. Stewart, G. R. Superconductivity in iron compounds. *Rev. Mod. Phys.* **83**, 1589–1652 (2011).
5. Ishida, K., Nakai, Y. & Hosono, H. To what extent iron-pnictide new superconductors have been clarified: A progress report. *J. Phys. Soc. Japan* **78**, 062001 (2009).
6. Pallecchi, I., Eisterer, M., Malagoli, A. & Putti, M. Application potential of Fe-based superconductors. *Supercond. Sci. Technol.* **28**, 114005 (2015).
7. Putti, M. *et al.* New Fe-based superconductors: Properties relevant for applications. *Supercond. Sci. Technol.* **23**, 034003 (2010).
8. Shimoyama, J. Potentials of iron-based superconductors for practical future materials. *Supercond. Sci. Technol.* **27**, 044002 (2014).
9. Tarantini, C. *et al.* Significant enhancement of upper critical fields by doping and strain in Fe-based superconductors. *Phys. Rev. B* **84**, 184522 (2011).
10. Wang, Z., Luo, H., Ren, C. & Wen, H. Upper critical field, anisotropy, and superconducting properties of Ba$_{1-x}$K$_x$Fe$_2$As$_2$ single crystals. *Phys. Rev. B* **78**, 140501 (2008).
11. Huang, H. *et al.* High transport current superconductivity in powder-in-tube Ba$_{0.6}$K$_{0.4}$Fe$_2$As$_2$ tapes at 27T. *Supercond. Sci. Technol.* **31**, 015017 (2018).
12. Togano, K. *et al.* Enhancement in transport critical current density of *ex situ* PIT Ag/(Ba, K)Fe$_2$As$_2$ tapes achieved by applying a combined process of flat rolling and uniaxial pressing. *Supercond. Sci. Technol.* **26**, 115007 (2013).
13. Yao, C. *et al.* Microstructure and transport critical current in Sr$_{0.6}$K$_{0.4}$Fe$_2$As$_2$ superconducting tapes prepared by cold pressing. *Supercond. Sci. Technol.* **26**, 075003 (2013).
14. Lin, H. *et al.* Hot pressing to enhance the transport J_c of Sr$_{0.6}$K$_{0.4}$Fe$_2$As$_2$ superconducting tapes. *Sci. Rep.* **4**, 6944 (2014).
15. Gao, Z. *et al.* Enhancement of practical level critical current densities in Ba$_{1-x}$K$_x$Fe$_2$As$_2$/Ag tapes by conventional cold mechanical deformation. *Sci. Rep.* **4**, 4065 (2014).
16. Lin, H. *et al.* Strongly enhanced current densities in Sr$_{0.6}$K$_{0.4}$Fe$_2$As$_2$ + Sn superconducting tapes. *Sci. Rep.* **4**, 4465 (2015).
17. Zhang, X. *et al.* Realization of practical level current densities in Sr$_{0.6}$K$_{0.4}$Fe$_2$As$_2$ tape conductors for high-field applications. *Appl. Phys. Lett.* **104**, 202601 (2014).
18. Pyon, S. *et al.* Improvements of fabrication processes and enhancement of critical current densities in (Ba, K)Fe$_2$As$_2$ HIP wires and tapes. *Supercond. Sci. Technol.* **31**, 055016 (2018).
19. Iyo, A. *et al.* Large critical current densities in a silver-sheathed (Sr, Na)Fe$_2$As$_2$ tape. *Supercond. Sci. Technol.* **28**, 105007 (2015).
20. Yao, C. *et al.* Improved transport critical current in Ag and Pb co-doped Ba$_x$K$_{1-x}$Fe$_2$As$_2$ superconducting tapes. *Supercond. Sci. Technol.* **25**, 035020 (2012).
21. Cortes-Gil, R., Parker, D. R., Pitcher, M. J., Hadermann, J. & Clarke, S. J. Indifference of superconductivity and magnetism to size-mismatched cations in the layered iron arsenides Ba$_{1-x}$Na$_x$Fe$_2$As$_2$. *Chem. Mater.* **22**, 4304–4311 (2010).
22. Tsuyoshi, T. *et al.* Demonstration of Excellent J_c Performance in (*AE*, Na)Fe$_2$As$_2$ (*AE*: Sr, Ba) PIT Wires. *IEEE Trans. Appl. Supercond.* **29**, 7300605 (2019).
23. Pyon, S., Yamasaki, Y., Kajitani, H. & Koizumi, N. Effects of drawing and high-pressure sintering on the superconducting properties of (Ba, K)Fe$_2$As$_2$ powder-in-tube wires. *Supercond. Sci. Technol.* **28**, 125014 (2015).
24. Lotgering, F. K. Topotactical reactions with ferrimagnetic oxides having hexagonal crystal structures-II. *J. Inorg. Nucl. Chem.* **16**, 100–108 (1960).
25. Ishida, S. *et al.* Fabrication of iron-based superconducting tapes using Ba$_{1-x}$K$_x$Fe$_2$As$_2$ with x = 0.3 and 0.4. *Supercond. Sci. Technol.* **30**, 054001 (2017).
26. Avci, S. *et al.* Structural, magnetic, and superconducting properties of Ba$_{1-x}$Na$_x$Fe$_2$As$_2$. *Phys. Rev. B* **88**, 094510 (2013).
27. Todorov, I. *et al.* Topotactic redox chemistry of NaFeAs in water and air and superconducting behavior with stoichiometry change. *Chem. Mater.* **22**, 3916–3925 (2010).
28. Shinohara, N. *et al.* Synthesis, structure, and phase diagram of (Sr$_{1-x}$Na$_x$)Fe$_2$As$_2$ superconductors. *Supercond. Sci. Technol.* **28**, 062001 (2015).
29. Awaji, S., Nakazawa, Y., Oguro, H. & Tsuchiya, Y. Anomalous anisotropy of critical currents in (Sr, K)Fe$_2$As$_2$ tapes. *Supercond. Sci. Technol.* **30**, 035018 (2017).
30. Gao, Z. *et al.* High transport J_c in stainless steel/Ag-Sn double sheathed Ba122 tapes. *Supercond. Sci. Technol.* **30**, 095012 (2017).
31. Togano, K., Gao, Z., Matsumoto, A. & Kumakura, H. Fabrication of (Ba, K)Fe$_2$As$_2$ tapes by *ex situ* PIT process using Ag-Sn alloy single sheath. *Supercond. Sci. Technol.* **30**, 015012 (2017).
32. Xianping, Z. *et al.* Realization of practical level current densities in Sr$_{0.6}$K$_{0.4}$Fe$_2$As$_2$ tape conductors for high-field applications. *Appl. Phys. Lett.* **104**, 202601 (2014).

Acknowledgements

Author Contributions

S. Ishida, T.N. and Y.Y. designed and coordinated the research plan. S. Imai, S. Itou, S. Ishida, Y.T., A.I. and K.M. carried out the superconducting tape fabrication and characterization. S. Imai and S. Itou wrote the main body of the manuscript under the support of other coauthors, particularly by H.E., T.N., and Y.Y. All authors contributed to the discussion of the results for the manuscript.

Additional Information

Competing Interests: The authors declare no competing interests.

Publisher's note: Springer Nature remains neutral with regard to jurisdictional claims in published maps and institutional affiliations.